HHS Public Access

Author manuscript

Colloids Surf B Biointerfaces. Author manuscript; available in PMC 2021 June 01.

Published in final edited form as:

Colloids Surf B Biointerfaces. 2020 June ; 190: 110938. doi:10.1016/j.colsurfb.2020.110938.

Physical-chemical interactions between dental materials surface, salivary pellicle and *Streptococcus gordonii*

Ting Sang[a,b], **Zhou Ye**[b], **Nicholas G. Fischer**[b], **Erik P. Skoe**[b], **Constanza Echeverría**[b,c], **Jun Wu**[a,*], **Conrado Aparicio**[b,*]

[a]The Affiliated Stomatological Hospital of Nanchang University & The Key Laboratory of Oral Biomedicine, Nanchang, Jiangxi Province, 330006, China

[b]MDRCBB, Minnesota Dental Research Center for Biomaterials and Biomechanics, University of Minnesota, Minneapolis, MN, 55455, USA

[c]Cariology Unit, Department of Oral Rehabilitation, University of Talca, Talca, 3460000, Chile

Abstract

Dental materials are susceptible to dental plaque formation, which increases the risk of biofilm-associated oral diseases. Physical-chemical properties of dental material surfaces can affect salivary pellicle formation and bacteria attachment, but relationships between these properties have been understudied. We aimed to assess the effects of surface properties and adsorbed salivary pellicle on *Streptococcus gordonii* adhesion to traditional dental materials. Adsorption of salivary pellicle from one donor on gold, stainless steel, alumina and zirconia was monitored with a quartz crystal microbalance with dissipation monitoring (QCM-D). Surfaces were characterized by X-ray photoelectron spectroscopy, atomic force microscopy and water contact angles measurement before and after pellicle adsorption. Visualization and quantification of Live/Dead stained bacteria and scanning electron microscopy were used to study *S. gordonii* attachment to materials with and without pellicle. The work of adhesion between surfaces and bacteria was also determined. Adsorption kinetics and the final thickness of pellicle formed on the four materials were similar. Pellicle deposition on all materials increased surface hydrophilicity, surface energy and work of adhesion with bacteria. Surfaces with pellicle had significantly more attached bacteria than surfaces without pellicle, but the physical-chemical properties of the dental material did not significantly alter bacteria attachment. Our findings suggested that the critical factor increasing *S. gordonii* attachment was the salivary pellicle formed on dental materials. This is attributed to increased work of adhesion between bacteria and substrates with pellicle. New dental materials

*Corresponding authors. wujundent@163.com (J. Wu), apari003@umn.edu (C. Aparicio).

CRediT authorship contribution statement

Ting Sang: Conceptualization, Validation, Formal analysis, Investigation, Data curation, Writing - original draft, Visualization. **Zhou Ye:** Methodology, Validation, Formal analysis, Investigation, Data curation, Writing - original draft, Visualization. **Nicholas G. Fischer:** Formal analysis, Investigation, Writing - review & editing. Erik **P. Skoe:** Investigation. **Constanza Echeverría:** Investigation. **Jun Wu:** Resources, Writing - review & editing, Funding acquisition. **Conrado Aparicio:** Conceptualization, Methodology, Formal analysis, Resources, Writing - review & editing, Visualization, Supervision, Funding acquisition.

Declaration of interests

The authors declare that they have no known competing financial interests or personal relationships that could have appeared to influence the work reported in this paper.

Data availability

The raw/processed data required to reproduce these findings will be made available on request.

should be designed for controlling bacteria attachment by tuning thickness, composition and structure of the adsorbed salivary pellicle.

Keywords

Bacteria adhesion; QCM-D; Work of adhesion; Surface energy; Dental biomaterials

1. Introduction

Dental materials are susceptible to dental plaque formation, which increases the risk of biofilm-associated oral diseases. Dental plaque biofilm is formed by a complex microbial community tightly bound to solid substrates including enamel and various dental materials [1,2]. Biofilm formation on orthodontic brackets and surrounding enamel can cause white spot lesions and/or dental caries. More than 73.5 % of orthodontic patients develop at least one new enamel white spot lesion at the time of bracket debonding [3]. Plaque accumulation on dental crowns may increase the occurrence of dental caries and periodontitis. The frequency of periodontitis in patients who have gone through crown restoration was reported as 14.4 % at 5 years [4]. Biofilm growth will shift the composition of the predominant species and alter the microecological balance with the host, which will further lead to disease onset [1,5]. Therefore, the development of dental materials with low susceptibility to bacterial attachment is of clear importance.

Some critical factors influencing dental plaque biofilm formation include surface charge, surface roughness (R_a), wettability, surface energy and substratum stiffness [6–10]. Most bacterial cells are negatively charged, thus negatively charged surfaces are generally more resistant to bacterial colonization [8]. Superhydrophobic and superhydrophilic surfaces can both prevent biofilm formation [11,12]. An increase in surface roughness promotes bacterial attachment due to the increase in contact area between the material surface and bacterial cells [10]. Microorganisms generally adhere more to a substrate with high surface energy than to a substrate with low surface energy [13]. Among these factors, surface roughness and surface energy have been regarded as the most important factors affecting biofilm formation [9]. Though many factors modulating the intrinsic properties of materials/bacteria interfaces have been investigated, correlations between surface properties and bacterial adhesion are yet not well understood [14].

Dental material surfaces are constantly exposed to saliva, which forms a surface conditioning film known as the acquired salivary pellicle. Acquired pellicle is a thin acellular film formed by selective adsorption of salivary proteins and glycoproteins on any type of surface upon exposure to saliva [15]. The initial conditioning stage of biofilm formation is the adhesion of the acquired pellicle [15,16]. Bacterial adherence to teeth or dental materials surfaces is mediated by the specific binding of bacterial surface adhesins to pellicle protein ligands [17]. Properties of the pellicle such as adsorbed mass [18], formation rate [19], morphology [20] and viscoelasticity [21] are dependent on the nature of the substratum on which it forms, but few studies have quantitatively compared the pellicle adsorption and its effect on bacterial attachment onto different dental materials.

Quartz crystal microbalance with dissipation monitoring (QCM-D) is a technique that enables real-time monitoring of adsorption/desorption and molecular interactions events of proteins and other analytes onto sensor surfaces. The combined measurements of changes in frequency and dissipation is used to calculate real-time changes in mass and viscoelasticity of the adsorbed protein layer [22–25]. QCM-D has been scarcely used to study development of varied salivary pellicle, its interactions with dental materials and/or oral rinsing solutions [21,26,27]. Previous work studying pellicle adsorption on dental materials or bacterial attachment using QCM-D [21,28–30] either did not establish relationships between salivary pellicle adsorption and bacterial attachment [21,29,30] or was limited to the investigation of a single dental/oral material (e.g. hydroxyapatite [26,27]).

Hence, our work aimed to unravel intrinsic physical-chemical properties of the substrates, salivary pellicles and bacteria that control and govern the oral bacterial attachment on dental materials, so that known relationships between these properties can instruct the design of new materials. Specifically, we assessed the effects of surface properties and adsorbed salivary pellicle on *Streptococcus gordonii* attachment to traditional dental materials, including two metals (gold, stainless steel) and two ceramics (aluminum oxide, zirconium oxide). *S. gordonii* is a primary colonizer of oral surfaces [31]. We used QCM-D and complementary characterization techniques to evaluate thickness, roughness, hydrophobicity and surface energy of the dental materials and the pellicle which formed on them. We also determined the work of adhesion between the different substrates and bacteria. Our first hypothesis was that the salivary pellicle thicknesses and adsorption kinetics are significantly different on different traditional dental materials. Our second hypothesis was that the work of adhesion between bacteria and adsorbed pellicle is significantly higher than between bacteria and material surfaces without pellicle, and thus the adsorbed pellicle increased attachment of *S. gordonii* bacteria compared to material surfaces without pellicle.

2. Materials and methods

2.1. Real-time monitoring of pellicle adsorption

2.1.1. Saliva collection—Unstimulated saliva was obtained from one researcher with good oral health by depositing saliva in a sterilized Falcon tube every minute until collection of 20 mL of saliva [21,32,33]. The salivary donor kept the same diet in the previous night and in the morning of the collection day to minimize the differences in saliva samples collected in different days. The saliva was immediately centrifuged twice at 35,280 RCF and 4 °C for 10 min. The supernatant was collected and filtered with 0.22 μm syringe filters (Millex™-GP Sterile Syringe Filters, MilliporeSigma™, USA). Then, the filtered saliva was diluted to 25 % (V/V) (FS) with autoclaved deionized (DI) water [21,33]. FS was used immediately for every experiment.

2.1.2. Adsorption of salivary pellicle—A QCM-D (Q-Sense E4 system, Biolin Scientific, Sweden) was used for monitoring the frequency and dissipation changes by flowing autoclaved DI water (control) or FS on QSensors (Biolin Scientific, Sweden) coated by the manufacturer with gold (Au; QSX-301), stainless steel (SS; QSX-304), aluminum oxide (Al_2O_3; QSX-309) and zirconium oxide (ZrO_2; QSX-330). The sensors were

thoroughly cleaned before QCM-D experiments following manufacturer instructions. Frequency and dissipation data were acquired with QSoft401 (version 2.6.1.712, Biolin Scientific, Sweden) and analyzed using QTool software (version 3.1.25.604, Biolin Scientific, Sweden). Measurements were taken at a constant temperature of 37 °C. Control groups were run with autoclaved DI water through the chambers at a flow rate of 0.2 mL/min until a stable baseline was reached (approximately 1 h). Experimental groups were run with autoclaved DI water at 0.2 mL/min for 1 h and then FS at 0.2 mL/min for 5 min, and 20 μL/min for 1 h, followed by autoclaved DI water at 0.2 mL/min for 30 min for rinsing loosely attached pellicle molecules. In each QCM-D experimental run, each of the four chambers contained one sensor with a different material coating and all chambers were exposed to the same saliva sample. Thus, assessment of the variations in adsorption of pellicle among the different materials would not be affected by the differences in saliva samples collected in different days.

The resonant frequency and the energy dissipation of the four sensors were continuously recorded to monitor real-time pellicle adsorption on the different coated sensors. The thickness of the formed pellicle was fit using the Kelvin-Voigt viscoelastic model. The pellicle layer was estimated to be homogeneous with a density of 1000 kg/m^3. The fluid density and viscosity of FS were estimated to be the same as water; 1000 kg/m^3 and 0.001 kg/m, respectively. The data were fitted from the 5^{th}, 7^{th} and 9^{th} overtones. All QCM-D experiments were performed four times.

2.2. Surface properties

2.2.1. Elemental composition—A X-ray photoelectron spectrometer (XPS; PHI 5000 Versa Probe III, ULVAC Inc, Kanagawa Japan) with a monochromatic Al Kα X-ray source (45°, 1486.6 eV, 50 W, sampling area: 200-μm diameter) was used to determine elemental composition of the four different sensor surfaces without and with pellicle. Survey spectra were collected at 0−1100 eV using a pass energy of 280 eV with a step size of 1.0 eV. Sensors were put into a desiccator to dry overnight prior to measurements. Each sensor was measured in 4 different locations with 15 scans per location.

2.2.2. Topography and roughness—Surfaces of the sensors without and with pellicle formed during QCM-D experiments were scanned in tapping mode using an atomic force microscope (AFM; Bruker Nanoscope V Multimode 8 AFM, Billerica, MA, USA) and silicon probes with tip radius of curvature < 10 nm and nominal force constant of 42 N/m (PPP-NCHR-10, Nanosensors, Neuchâtel, Switzerland). The scanning rate was 1 Hz and the scanning area was 1 μm × 1 μm. Roughness (R_a) was calculated using Gwyddion software (version 2.52, gwyddion.net).

2.2.3. Wettability—Water contact angles (WCA) on Au, SS, Al_2O_3, ZrO_2 sensors without and with pellicle formed during QCM-D experiments were determined using the sessile drop method with a contact angle goniometer (DMCE1, Kyowa Interface Science, Japan) and FAMAS software (Kyowa Interface Science, Japan). A 2 μL droplet of deionized (DI) water was deposited on the tested surface and tracked for 60 s. Measurements were repeated four times at different locations on each surface.

2.2.4. Surface energy—To calculate the solid-vapor surface energies (γ_{SV})of each surface and their polar and dispersive components (γ_S^p, γ_S^d, respectively), contact angles with formamide and diiodomethane were determined in the same way as described for WCA. The surface energies of the three liquids and their polar and dispersive components (γ_{LV}, $\gamma_L^p\gamma_L^d$, respectively) were obtained from [34]. The relationships between the solid surface energies and liquid surface energies follow the following equations [35].

$$\gamma_{SL} = \gamma_{SV} + \gamma_{LV} - 2\left(\gamma_S^p\gamma_L^p\right)^{1/2} - 2\left(\gamma_S^d\gamma_L^d\right)^{1/2} \quad (1)$$

$$\gamma_{SV} = \gamma_{SL} + \gamma_{LV}\cos\theta \quad (2)$$

$$\gamma_{SV} = \gamma_S^p + \gamma_S^d \quad (3)$$

$$\gamma_{LV} = \gamma_L^p + \gamma_L^d \quad (4)$$

After combining these equations, the unknown parameters (γ_S^p and γ_S^d) can be calculated from the following equation [36]:

$$\gamma_{LV}(1+\cos\theta)/2\left(\gamma_L^d\right)^{1/2} = \left(\gamma_S^p\right)^{1/2}\left(\gamma_L^p/\gamma_L^d\right)^{1/2} + \left(\gamma_S^d\right)^{1/2} \quad (5)$$

In the linear fitting of $\gamma_{LV}(1+\cos\theta)/2\left(\gamma_L^d\right)^{1/2}$ vs $\left(\gamma_L^p/\gamma_L^d\right)^{1/2}$, the slope is $\left(\gamma_S^p\right)^{1/2}$ and the intercept is $\left(\gamma_S^d\right)^{1/2}$. The total surface energy of each sensor (γ_{SV}) is then calculated from Eq. (3).

2.3. Bacterial attachment

2.3.1. Bacteria growth and attachment to surfaces—The strain *S. gordonii* M5 was cultured on Brain Heart Infusion (BHI, BD Difco, USA) agar plates at 37 °C in aerobic condition for 48 h followed by incubation in Todd Hewitt Broth medium (THB, BD Difco, USA) at 37 °C in aerobic condition with a shaking speed of 150 rpm until OD_{600} of 0.20 was reached (approximately 6 h).

The sensors coated with dental materials with and without adsorbed pellicle were conditioned in a 12 well-plate with THB medium at 37 °C for 0.5 h immediately after removal from the QCM-D chambers. The bacterial solution was diluted to OD_{600} of 0.02. All the sensors were immersed into the bacterial solution and incubated for 6 h with a shaking speed of 150 rpm.

2.3.2. Quantification by imaging of attached bacteria—A LIVE/DEAD assay was performed to visualize bacteria colonization on sensors. After bacterial culture, sensors were washed in phosphate-buffered saline (PBS) and stained at room temperature in SYTO©9

and propidium iodide in PBS following the manufacturer's instructions (LIVE/DEAD™ *Bac*Light™ Bacterial Viability Kit, Thermo Fisher Scientific, Waltham, MA, USA). Bacteria with an intact membrane fluoresce green, whereas bacteria with a compromised membrane fluoresce red. Micrographs were obtained with a confocal laser scanning microscope (CLSM; FluoView FV1000, Olympus) at ×20 (NA = 0.85) at constant settings across all sensors. Micrograph analysis and visualization were performed in Fiji-ImageJ (NIH, https://imagej.net/Fiji). Because almost all bacteria were live, bacterial covered surface area (in pixels) was calculated by binarizing the green (SYTO©9) channel and calculating the SYTO©9-positive number of pixels. Nine fields of view (arranged in a 3 ×3 grid where each field was 2 mm apart) were collected from four separate experiments for each surface.

2.3.3. Visualization of attached bacteria—Sensors with attached bacteria were prepared for field-emission scanning electron microscopy (SEM; Hitachi SU8230, Tokyo, Japan) imaging following the methods described elsewhere [37]. Briefly, after being incubated in bacterial culture solutions, the sensors were first washed gently in PBS to remove loosely attached bacteria. The attached bacteria were then fixed in a 2.5 % glutaraldehyde solution in PBS for 2 h at 4 °C. The fixed sensors were washed in PBS for 20 min twice and in DI water for 20 min twice. The washed sensors were serially dehydrated in 35 %, 50 %, 75 % and 95 % ethanol for 30 min each and in 100 % ethanol 3 times ×30 min. Then the sensors with attached bacteria were dried using a CO_2 critical-point dryer (Model 780A, Tousimis, Rockville, MD, USA). The dried specimens were sputter-coated with a 5 nm thick iridium layer. The attached bacteria were imaged at an accelerating voltage of 5 kV.

2.3.4. Surface energy of bacteria layers—The contact angles of DI water, formamide and diiodomethane were measured on a thick layer of *S. gordonii* deposited on membrane filters [38]. *S. gordonii* was incubated overnight until OD_{600} of 1.62. Bacteria solution was centrifuged at 5000 RCF for 5min and re-suspended in DI water three times. A total of 5 mL of washed bacteria solution was passed through a 25 mm mixed cellulose esters membrane with 0.45 μm pore size (HAWP02500, Millipore Sigma, Darmstadt, Germany). The membranes with collected bacteria were kept in moisture on a BHI agar plate and measured within 30 min. Contact angles with each liquid were measured on three membranes with bacteria. The surface energy of *S. gordonii* was calculated using the same method described for the sensors.

2.4. Evaluation of work of adhesion between surfaces and bacteria

After obtaining the surface energies of sensors, sensors with pellicle and *S. gordonii*, the work of adhesion (W_{ad}) between the different sensor surfaces and *S. gordonii* was calculated from the equation below [35]:

$$W_{ad} = 2\left(\gamma_S^p \gamma_B^p\right)^{1/2} + 2\left(\gamma_S^d \gamma_B^d\right)^{1/2} \quad (6)$$

Where γ_S^p and γ_S^d are the surface energy polar and dispersive components, respectively, of the sensor surface and γ_B^p and γ_B^d are the surface energy polar and dispersive components, respectively, of bacteria layers.

2.5. Statistical analysis

Statistical analysis was performed using SPSS software (version 17.0, SPSS Inc., Chicago, USA). Kolmogorov-Smirnov test was used to assess normality and Levene's test was used to assess homogeneity of variances among tested groups. Then, statistically significant differences between groups (p-value < 0.05) were determined using Welch's ANOVA with Tukey post-hoc test, Kruskal Wallis test and Welch's ANOVA with the Dunnett T3 post hoc test for pellicle thickness, WCA and number of attached bacteria, respectively.

3. Results

3.1. Real-time monitoring of pellicle adsorption

The changes in frequency (ΔF) and changes in energy dissipation (ΔD) vs time were plotted to monitor salivary pellicle adsorption on coated sensors (Fig. 1). After initial stabilization of the system in water, a large and rapid drop in ΔF of about −45 Hz within 5 min was observed for the four dental materials (Fig. 1, arrow 'Filtered saliva') when they were exposed to FS. This drop was indicative of the rapid absorption of molecules from FS to form a pellicle onto the tested surfaces. Thereafter, ΔF was stable over time of exposure to FS. Simultaneous to the drop in ΔF, a corresponding increase in ΔD to a stable level within 5 min was assessed. The sensors were then rinsed with water (Fig. 1a, arrow 'Water rinse' at 65 min). A small increase in ΔF was detected over a short period of 2 min, whereas a simultaneous relatively large decrease in ΔD indicated that the pellicle was more compact, and thus only loosely attached pellicle molecules were removed from the sensor surface during water rising. ΔF and ΔD evolution and values were similar among these four dental material surfaces during all steps of the experiment.

To quantify the salivary pellicle formation in real-time, pellicle thickness over time was calculated using the Kelvin-Voigt viscoelastic model based on the 5th, 7th and 9th overtones of QCM-D frequency and dissipation changes (Fig. 2). Pellicle thickness increased rapidly to 12−15 nm on all four surfaces within 5 min after exposure to FS (Fig. 2a, arrow 'Filtered saliva'). Pellicle thicknesses were stable over the following 60 min; i.e., before water rinse (Fig. 2a, arrow 'Water rinse'). During water rinse, the pellicle thicknesses decreased rapidly within 2 min as the loosely attached molecules in the formed pellicle layer were removed. Fig. 2b shows the average pellicle thickness formed on the four dental materials before and after water rinse. No statistically significant differences in pellicle thickness were determined between the four different sensor surfaces both before and after water rinse.

3.2. Surface properties

The surface elemental composition of the sensors before and after pellicle adsorption was detected and quantified by XPS (Fig. 3). All characteristic elemental XPS peaks of each coated sensor were identified. The intensities of N1s and C1s peaks significantly increased

after pellicle adsorption on the sensor surfaces while the intensities of the signature peaks from the sensor materials (Au, Fe, Al, Zr) diminished. As a result, the ratio of C/metal element and N/metal element strikingly increased, which confirmed the thorough coverage of the sensors by the adsorbed pellicle.

AFM was used to characterize the surface topography of the four coated sensors before and after the QCM-D experiment (Fig. 4). The adsorbed pellicle had similar topographical features on Au, SS and Al_2O_3 sensors. Pellicle on ZrO_2 sensors had larger and less uniform protein agglomerates than on the other three sensors. Before depositing saliva, all four sensors had similar values of roughness (R_a < 1.0 nm), which did not change after pellicle adsorption except for pellicle on the ZrO_2 sensor (R_a =1.8 nm).

Surface hydrophobicity of the four sensors before and after QCM-D experiment was evaluated by WCA and is summarized in Table 1. SS and ZrO_2 sensors were the most hydrophilic and most hydrophobic, respectively. Only these two groups had statistically different WCA. Surfaces with pellicle were statistically more hydrophilic than the corresponding surfaces without pellicle. However, no significant differences were determined between the different sensors after being covered with pellicle (Table 1).

The calculated surface energies were consistent with the WCA measurements (Table 1). Before depositing the pellicle layer, SS and ZrO_2 sensors had the highest and the lower surface energy polar component (γ_S^p), respectively. The presence of the pellicle on the sensors notably increased γ_S^p and overall surface energy (γ_{SV}) when compared with the four sensors without pellicle, which contributed to the higher hydrophilicity of the pellicle-coated surfaces.

3.3. Bacterial attachment

CLSM of Live/Dead staining and SEM were used to visualize and quantify the bacterial attachment on each sensor surface before and after pellicle adsorption. Representative CLSM images of the attached bacteria showed that most of the visual field was green (live) and a red (dead) area was rarely detected after Live/Dead fluorescence staining (Fig. 5a). As almost only a monolayer of bacteria was formed in this early stage biofilm formation, the surface area covered by bacteria (in pixels) was used to quantitatively compare the bacterial attachment (Fig. 5b). A significantly higher number of bacteria attached to the surfaces with pellicle was detected compared to surfaces without pellicle, whereas no significant differences on attached bacteria were observed between the four sensor surfaces with pellicle. Notably, the bacteria attached on the sensors without pellicle was almost negligible on all sensors, except on SS sensors.

SEM micrographs revealed morphological details of the attached *S. gordonii* on the different substrates (Fig. 6). Only isolated *S. gordonii* bacteria and/or chains of bacteria were visualized on the sensors without pellicle. In contrast, much more bacteria were attached in large colonies on the sensors with pellicle. The SEM micrographs also demonstrated that there was no distinct difference in the number of bacteria between the four sensor surfaces with or without pellicle.

3.4. Work of adhesion between sensor surfaces and S. gordonii

The work of adhesion (W_{ad}) between the surface of SS sensors and *S. gordonii* was the highest among all sensors before pellicle adsorption (Table 1) as SS sensors had the highest surface energy polar component. The higher W_{ad} for SS sensor might be correlated to the better attachment of bacteria to these sensors, compared to the other three sensors (Fig. 5a). The W_{ad} increased 30–40 mJ/m^2 on all sensors after pellicle adsorption and was similar for all pellicle formed on the four materials.

Overall, these results indicated that the different physical-chemical properties of the dental materials tested did not result in significantly different physical-chemical properties of the pellicle formed on them. Moreover, the work of adhesion between the surface and bacteria can be a predictor of bacteria attachment.

4. Discussion

Bacterial attachment and accumulation on dental materials, such as orthodontic brackets and dental crowns, can cause many oral diseases. Acquired enamel pellicle protects the tooth from erosive wear. On the other hand, salivary pellicle formed on dental material surfaces facilitates the bacterial attachment and biofilm growth. Our work studied the physical-chemical interactions between salivary pellicle and four traditional dental materials (i.e., Au, SS, Al_2O_3 and ZrO_2). We further evaluated the effect of pellicle adsorption on *S. gordonii* attachment and explored the effects of the work of adhesion between bacteria and dental materials or pellicle in bacteria attachment.

The small, but significant differences in wettability and other physicochemical properties between the four dental materials tested here did not result in significant differences in either the kinetics of adsorption of salivary pellicle nor the final pellicle thicknesses formed on these materials. Others have shown similar results. Pioneer work by Hannig reported no morphological nor thickness differences between salivary pellicles formed on enamel compared to resin composites, amalgams, and casting alloys [39] and others showed no morphological differences between salivary pellicles on microfilled composites and glass ionomers [40]. The formation of the acquired pellicle proceeds through selective adsorption of salivary proteins and additional lipids and glycoproteins [41]. *in vivo*, the initial phase of pellicle formation occurs within seconds [42], during which precursor proteins, such as statherin, acidic proline-rich proteins and histatins preferentially adhere to the surface, forming a thin protein layer [43]. Then a rapid accumulation forms a thick pellicle during the second stage of pellicle formation. Adsorption of large, knotted, globular structures occurs in this phase and suggests that protein aggregates (micelle-like structures), rather than individual proteins, are responsible for subsequent pellicle development [44]. These protein aggregates are known to be primarily composed of mucin MG1 associated with - among others -statherin, cystatins and lysozyme [45,46]. Thus, the final thickness of the pellicle seems to be dominated by the second stage of adsorption of the pellicle, where the substrate does not have the ability to directly and therefore selectively interact with the adsorbed molecular aggregates [43]. This may explain the lack of differences in thickness and roughness/structure of the pellicles we obtained here and suggests that specific effects that different substrates can have on selective adsorption of proteins to form the basal layer of the

pellicle might not be relevant to affect the overall structure/thickness of the pellicle and its final surface physical-chemical-properties. Our results further suggested that dental materials with quite different chemical natures cannot directly affect bacteria attachment in the oral environment as they did not notably affect the physical-chemical properties of the acquired pellicle. This was further supported in our study as: first, the formed salivary pellicle significantly increased the attachment of *S. gordonii* to all dental materials; and second, the attachment of bacteria was similar to all pellicle-coated surfaces, irrespective of the material on which the pellicle was formed. Indeed, SS had significantly higher hydrophilicity and attached bacteria than any other dental material; however, these differences were eliminated after formation of the pellicle. Overall, our results indicated that the acquired pellicle, and not the dental material, was the critical factor favoring the adhesion of *S. gordonii* bacteria.

We focused on the role of surface energy and eliminated the effect of roughness [9] by using thin-film coated QCM-D sensors, which all had values of roughness as low as $R_a < 1$nm. Others have shown that surface energy is the driving factor for adhesion of microorganisms to the substrate surfaces and that the lower the surface energy of the substrate, the weaker the work of adhesion between bacteria and surfaces [47,48]. The work of adhesion is defined as the work required to separate one substance (i.e., bacteria) from the substrate (i.e., sensor surface). Results from our experiments showed that all the polar components of the surface energies increased after acquisition of the pellicle, which indicated that the presence of the pellicle increased the polarity of all materials surfaces. This is because the proteins and enzymes in saliva contain a large amount of polar amino acids that, once adsorbed on the substrate [49], are exposed at the surface/water interface. As the surface of the *S. gordonii* layers was also highly polar, the work of adhesion between the bacteria and the substrates tested here consistently increased after pellicle adsorption. Increasing work of adhesion implies that it was more difficult for the bacteria to detach from pellicle than from uncoated dental materials, resulting in more bacterial retention on surfaces with adsorbed salivary components. Schweikl et al. [50] also concluded that functional groups added by the adsorption of specific salivary proteins to material surfaces are more relevant for initial bacterial adhesion than hydrophobicity as a physical property of the material.

Here we assessed similar *S. gordonii* bacteria attachment on the four materials after pellicle formation, and found a relationship with the fact that the pellicle reduced the intrinsic differences in physical-chemical properties of the materials. This was a surprising outcome as there is evidence of differences in salivary pellicle composition at the amino acid [51] and the protein level [52] depending on the nature of the dental material in which the pellicle is formed. We did not investigate here differences in composition of the pellicle formed on the different materials tested, but based on previous works we should expect compositional differences between them. However, as discussed above, the rapid and unspecific adsorption of molecules in the formation of agglomerates during the second stage of formation of the pellicle might render a pellicle surface with physical-chemical properties that are not significantly affected by the sometimes subtle differences in the bulk composition of the pellicle. In addition, many proteins in the salivary pellicle, such as MG2, amylase, and the acidic proline-rich proteins provide binding sites for *S. gordonii* [53]. This may trigger additional specific biomolecular interactions between bacteria and pellicle, favoring bacteria

colonization of the surfaces beyond the effects of nonspecific van der Waals and electrostatic properties determined here.

Much new dental material development has targeted reduction of bacterial attachment by modifying surface physical-chemical properties and/or implementing antifouling/antibacterial coatings [54]. However, our results suggest that the nonspecific acquisition of the salivary pellicle might effectively coat the engineered surfaces and so mask the designed physical, chemical and/or biological effects of these surfaces. Consequently, future innovations should focus on the control and assessment of the interaction between the surface of dental materials and the acquired pellicle formed on them. Promising dental materials should have the ability of eradicating/reducing, as well as modulating, the structure and composition of the acquired pellicle layer. Surface modifications have been explored to modulate the adsorption of salivary pellicles on dental materials, such as competitive adsorption of polyelectrolytes [28], dendrimer-grafted coating [55], and protein-repellant monomer addition to dental restorative resins [56]. Hydrophilic PEG modified surfaces have proved to reduce the mass of the pellicle formed from human whole saliva [57]. The main goal of these modifications has been generating an antifouling surface, inspired by the large body of literature on antifouling surfaces [58], which weakens the binding of the salivary proteins. Modulation of specific salivary pellicle components adsorption is difficult due to the large number of salivary proteins competing for adsorption to form the pellicle [59] and indeed, has been minimally explored [60], but may prove advantageous for controlling pellicle formation and eventual biofilm growth. Different dental materials can influence the protein profile of the salivary pellicle formed on them [52], but the specific proteins that regulate bacteria attachment are still a highly active area of research. One potential candidate to be specifically targeted is statherin as this protein is not only prevalent in the pellicle basal layer but also has constant relative abundance in all time-points during formation of the natural pellicle [49].

The oral biofilm formation is a complex process, which includes the formation of acquired pellicle and the initial adhesion of many bacterial species (e.g., Actinomyces spp, Streptococcusspp, Haemophilusspp, Capnocytophagaspp, Veillonellaspp, and Neisseria) [61]. The salivary pellicle layer might have different effects on other bacteria even though *S. gordonii* is a primary colonizer. Moreover, after the initial attachment of bacteria, they start to secrete extracellular polymeric substances, which further modify the materials surfaces. We did not explore the maturation stage of the biofilm formation and focused on the initial stage of attachment of bacteria to the substrates (6 h) considering that the dental materials we studied are used to make orthodontic appliances or restorative materials and meant to be cleaned daily. However, this study only used one bacteria strain as a model for bacteria attachment to substrates. Future studies should investigate biofilm formation under more clinically relevant and simulative conditions, such as using multispecies bacteria or clinically-obtained samples of microcosm biofilms.

5. Conclusions

Adsorption kinetics and final thickness of salivary pellicle formed on the four tested traditional dental materials were similar, and thus we rejected our first hypothesis. Our

second hypothesis was validated as pellicle deposition on all dental materials increased surface hydrophilicity, surface energy and work of adhesion with bacteria; and surfaces with pellicle had significantly more attached bacteria than surfaces without pellicle. On the contrary, the differences in physical-chemical properties of the dental materials had no notable effects on bacterial attachment. Therefore, the critical factor increasing *S. gordonii* attachment was the salivary pellicle formed on the dental materials. This is attributed to the significantly increased work of adhesion between bacteria and substrates with pellicle. Our results strongly suggest that new dental materials should be designed for controlling bacteria attachment by tuning thickness, composition and structure of the adsorbed salivary pellicle.

Acknowledgements

The authors acknowledge Dr. Ian Huxford, University of Minnesota, for helpful discussion on designing the QCM-D experiment and Dr. Bhaskar Valamakanni, 3M Oral Care, for providing access to the QCM-D equipment. CLSM imaging and analysis was performed at the University Imaging Centers, University of Minnesota. Parts of this work were carried out in the Characterization Facility, University of Minnesota, which receives partial support from NSF through the MRSEC program. This work was supported by the Jiangxi Provincial Department of Science and Technology, China [grant number 20171BEI90008 to J.W.], [grant number 20192BBG70022 to T.S.]; Hundred People Voyage Project of Jiangxi Association for Science and Technology [grant number (2017) 91 to T.S.]; and 3M Gives [Key Opinion Leaders Scholarship to C.E]. This research was supported by the National Institutes of Health's National Center for Advancing Translational Sciences [Translational Research Development Program-TRDP award to Z.Y. from grant UL1TR002494]. The content is solely the responsibility of the authors and does not necessarily represent the official views of the National Institutes of Health's National Center for Advancing Translational Sciences.

References

[1]. Sbordone L, Bortolaia C, Oral microbial biofilms and plaque-related diseases: microbial communities and their role in the shift from oral health to disease, Clin. Oral Investig. (2003), 10.1007/s00784-003-0236-1.

[2]. Colombo APV, Tanner ACR, The role of bacterial biofilms in dental caries and periodontal and peri-implant diseases: a historical perspective, J. Dent. Res. (2019), 10.1177/0022034519830686.

[3]. Enaia M, Bock N, Ruf S, White-spot lesions during multibracket appliance treatment: a challenge for clinical excellence, Am. J. Orthod. Dentofacial Orthop. (2011), 10.1016/j.ajodo.2010.12.016.

[4]. Behr M, Zeman F, Baitinger T, Galler J, Koller M, Handel G, Rosentritt M, The clinical performance of porcelain-fused-to-Metal precious alloy single crowns: chipping, recurrent caries, periodontitis, and loss of retention, Int. J. Prosthodont. (2014), 10.11607/ijp.3440.

[5]. Sanz M, Beighton D, Curtis MA, Cury JA, Dige I, Dommisch H, Ellwood R, Giacaman R, Herrera D, Herzberg MC, Könönen E, Marsh PD, Meyle J, Mira A, Molina A, Mombelli A, Quirynen M, Reynolds EC, Shapira L, Zaura E, Role of microbial biofilms in the maintenance of oral health and in the development of dental caries and periodontal diseases. Consensus report of group 1 of the Joint EFP/ORCA workshop on the boundaries between caries and periodontal disease, J. Clin. Periodontol. (2017), 10.1111/jcpe.12682.

[6]. Badihi Hauslich L, Sela MN, Steinberg D, Rosen G, Kohavi D, The adhesion of oral bacteria to modified titanium surfaces: role of plasma proteins and electrostatic forces, Clin. Oral Implants Res. (2013), 10.1111/j.1600-0501.2011.02364.x.

[7]. Busscher HJ, Rinastiti M, Siswomihardjo W, Van Der Mei HC, Biofilm formation on dental restorative and implant materials, J. Dent. Res. (2010), 10.1177/0022034510368644.

[8]. Song F, Koo H, Ren D, Effects of material properties on bacterial adhesion and biofilm formation, J. Dent. Res. (2015), 10.1177/0022034515587690.

[9]. Teughels W, Van Assche N, Sliepen I, Quirynen M, Effect of material characteristics and/or surface topography on biofilm development, Clin. Oral Implants Res (2006), 10.1111/j.1600-0501.2006.01353.x.

[10]. Anselme K, Davidson P, Popa AM, Giazzon M, Liley M, Ploux L, The interaction of cells and bacteria with surfaces structured at the nanometre scale, Acta Biomater. (2010), 10.1016/j.actbio.2010.04.001.

[11]. Zhang X, Wang L, Levänen E, Superhydrophobic surfaces for the reduction of bacterial adhesion, RSC Adv (2013), 10.1039/c3ra40497h.

[12]. Mi L, Jiang S, Integrated antimicrobial and nonfouling zwitterionic polymers, Angew. Chemie - Int. Ed (2014), 10.1002/anie.201304060.

[13]. Quirynen M, Bollen CML, The influence of surface roughness and surface-free energy on supra- and subgingival plaque formation in man: A review of the literature, J. Clin. Periodontol (1995), 10.1111/j.1600-051X.1995.tb01765.x.

[14]. Hahnel S, Rosentritt M, Handel G, Bürgers R, Surface characterization of dental ceramics and initial streptococcal adhesion in vitro, Dent. Mater. (2009), 10.1016/j.dental.2009.02.003.

[15]. Siqueira WL, Custodio W, McDonald EE, New insights into the composition and functions of the acquired enamel pellicle, J. Dent. Res. (2012), 10.1177/0022034512462578.

[16]. Lendenmann U, Grogan J, Oppenheim FG, Saliva and dental pellicle–a review, Adv. Dent. Res. (2000), 10.1177/08959374000140010301.

[17]. Whittaker CJ, Klier CM, Kolenbrander PE, Mechanisms of adhesion by ORAL BACTERIA, Annu. Rev. Microbiol. (2002), 10.1146/annurev.micro.50.1.513.

[18]. Vassilakos N, Arnebrant T, O Glantz P, Adsorption of whole saliva onto hydrophilic and hydrophobic solid surfaces: influence of concentration, ionic strength and pH, Eur. J. Oral Sci. (1992), 10.1111/j.1600-0722.1992.tb01085.x.

[19]. Vassilakos N, Arnebrant T, P. -O Glantz, An in vitro study of salivary film formation at solid/liquid interfaces, Eur. J. Oral Sci. (1993), 10.1111/j.1600-0722.1993.tb01652.x.

[20]. Schwender N, Huber K, Al Marrawi F, Hannig M, Ziegler C, Initial bioadhesion on surfaces in the oral cavity investigated by scanning force microscopy, in: Appl. Surf. Sci. (2005), 10.1016/j.apsusc.2005.02.042.

[21]. Barrantes A, Arnebrant T, Lindh L, Characteristics of saliva films adsorbed onto different dental materials studied by QCM-D, Colloids Surf. A Physicochem. Eng. Asp (2014), 10.1016/j.colsurfa.2013.05.054.

[22]. Alexander TE, Lozeau LD, Camesano TA, QCM-D characterization of time-dependence of bacterial adhesion, Cell Surf. 5 (2019) 100024,, 10.1016/j.tcsw.2019.100024. [PubMed: 32743140]

[23]. Alassi A, Benammar M, Brett D, Quartz crystal microbalance electronic interfacing systems: a review, Sensors (Switzerland) (2017), 10.3390/s17122799.

[24]. Scheideler L, Rupp F, Wendel HP, Sathe S, Geis-Gerstorfer J, Photocoupling of fibronectin to titanium surfaces influences keratinocyte adhesion, pellicle formation and thrombogenicity, Dent. Mater. (2007), 10.1016/j.dental.2006.03.005.

[25]. Höök F, Kasemo B, Nylander T, Fant C, Sott K, Elwing H, Variations in coupled water, viscoelastic properties, and film thickness of a Mefp-1 protein film during adsorption and cross-linking: A quartz crystal microbalance with dissipation monitoring, ellipsometry, and surface plasmon resonance study, Anal. Chem. (2001), 10.1021/ac0106501.

[26]. Ash A, Burnett GR, Parker R, Ridout MJ, Rigby NM, Wilde PJ, Structural characterisation of parotid and whole mouth salivary pellicles adsorbed onto DPI and QCMD hydroxyapatite sensors, Colloids Surf. B Biointerfaces (2014), 10.1016/j.colsurfb.2013.10.024.

[27]. Santos O, Lindh L, Halthur T, Arnebrant T, Adsorption from saliva to silica and hydroxyapatite surfaces and elution of salivary films by SDS and delmopinol, Biofouling (2010), 10.1080/08927014.2010.506609.

[28]. Lee HS, Myers C, Zaidel L, Nalam PC, Caporizzo MA, Daep CA, Eckmann DM, Masters JG, Composto RJ, Competitive adsorption of polyelectrolytes onto and into pellicle-coated hydroxyapatite investigated by QCM-D and force spectroscopy, ACS Appl. Mater. Interfaces (2017), 10.1021/acsami.7b02774.

[29]. Olsson ALJ, Van Der Mei HC, Busscher HJ, Sharma PK, Influence of cell surface appendages on the bacterium-substratum interface measured real-time using QCM-D, Langmuir (2009), 10.1021/la803301q.

[30]. Tam K, Kinsinger N, Ayala P, Qi F, Shi W, Myung NV, Real-time monitoring of streptococcus mutans biofilm formation using a quartz crystal microbalance, Caries Res (2007), 10.1159/000108321.

[31]. Li J, Helmerhorst EJ, Leone CW, Troxler RF, Yaskell T, Haffajee AD, Socransky SS, Oppenheim FG, Identification of early microbial colonizers in human dental biofilm, J. Appl. Microbiol. (2004), 10.1111/j.13652672.2004.02420.x.

[32]. Macakova L, Yakubov GE, Plunkett MA, Stokes JR, Influence of ionic strength changes on the structure of pre-adsorbed salivary films. A response of a natural multi-component layer, Colloids Surf. B Biointerfaces (2010), 10.1016/j.colsurfb.2009.12.022.

[33]. Alenus J, Ethirajan A, Horemans F, Weustenraed A, Csipai P, Gruber J, Peeters M, Cleij TJ, Wagner P, Molecularly imprinted polymers as synthetic receptors for the QCM-D-based detection of l-nicotine in diluted saliva and urine samples, Anal. Bioanal. Chem. (2013), 10.1007/s00216-0137080-1.

[34]. Wu S, Polymer Interface and Adhesion, 1st ed., Routledge, New York, 2017, 10.1201/9780203742860.

[35]. Owens DK, Wendt RC, Estimation of the surface free energy of polymers, J. Appl. Polym. Sci. (1969), 10.1002/app.1969.070130815.

[36]. Ye Z, Kim A, Mottley CY, Ellis MW, Wall C, Esker AR, Nain AS, Behkam B,Design of Nanofiber Coatings for Mitigation of Microbial Adhesion: Modeling and Application to Medical Catheters, ACS Appl. Mater. Interfaces (2018), 10.1021/acsami.8b02907.

[37]. Ye Z, Ellis MW, Nain AS, Behkam B, Effect of electrode sub-micron surface feature size on current generation of Shewanella oneidensis in microbial fuel cells, J. Power Sources (2017), 10.1016/j.jpowsour.2017.02.032.

[38]. Busscher HJ, Weerkamp AH, van Der Mei HC, van Pelt AW, de Jong HP, Arends J, Measurement of the surface free energy of bacterial cell surfaces and its relevance for adhesion, Appl. Environ. Microbiol. (1984).

[39]. Hannig M, Transmission electron microscopic study of in vivo pellicle formation on dental restorative materials, Eur. J. Oral Sci. (1997), 10.1111/j.1600-0722.1997.tb02139.x.

[40]. Shahal Y, Steinberg D, Hirschfeld Z, Bronshteyn M, Kopolovic K, In vitro bacterial adherence onto pellicle-coated aesthetic restorative materials, J. Oral Rehabil. 25 (1998) 52–58. [PubMed: 9502127]

[41]. DAWES C, The nomenclature of the integuments of the enamel surface of tooth, Br. Dent. Nurs. J. 115 (1963) 65–68 (Accessed February 3, 2020), http://ci.nii.ac.jp/naid/20000977685/en/.

[42]. Hannig M, Balz M, Influence of in vivo formed salivary pellicle on enamel erosion, Caries Res (1999), 10.1159/000016536.

[43]. Hannig M, Joiner A, The structure, function and properties of the acquired pellicle, Monogr. Oral Sci (2006), 10.1159/000090585.

[44]. Hannig M, Herzog S, Willigeroth SF, Zimehl R, Atomic force microscopy study of salivary pellicles formed on enamel and glass in vivo, Colloid Polym. Sci. (2001), 10.1007/s003960000478.

[45]. Iontcheva I, Oppenheim FG, Troxler RF, Human salivary mucin MG1 selectively forms heterotypic complexes with amylase, proline-rich proteins, statherin, and histatins, J. Dent. Res. (1997), 10.1177/00220345970760030501.

[46]. Vukosavljevic D, Custodio W, Buzalaf MAR, Hara AT, Siqueira WL, Acquired pellicle as a modulator for dental erosion, Arch. Oral Biol. (2014), 10.1016/j.archoralbio.2014.02.002.

[47]. Weerkamp AH, Uyen HM, Busscher HJ, Effect of zeta potential and surface energy on bacterial adhesion to uncoated and saliva-coated human enamel and dentin, J. Dent. Res. (1988), 10.1177/00220345880670120801.

[48]. Lindner E, Arias E, Surface Free Energy Characteristics of Polyfluorinated Silane Films, Langmuir (1992), 10.1021/la00040a029.

[49]. Lee YH, Zimmerman JN, Custodio W, Xiao Y, Basiri T, Hatibovic-Kofman S, Siqueira WL, Proteomic evaluation of acquired enamel pellicle during in vivo formation, PLoS One (2013), 10.1371/journal.pone.0067919.

[50]. Schweikl H, Hiller KA, Carl U, Schweiger R, Eidt A, Ruhl S, Müller R, Schmalz G, Salivary protein adsorption and Streptococccus gordonii adhesion to dental material surfaces, Dent. Mater. (2013), 10.1016/j.dental.2013.07.021.

[51]. Öste R, Rönström A, Birkhed D, Edwardsson S, Stenberg M, Gas-liquid chromatographic analysis of amino acids in pellicle formed on tooth surface and plastic film in vivo, Arch. Oral Biol. (1981), 10.1016/0003-9969(81)90159-X.

[52]. Pelá VT, Prakki A, Wang L, Ventura TMS, deSouza eSilva CM, Cassiano LPS, Brianezzi LFF, Leite AL, Buzalaf MAR, The influence of fillers and protease inhibitors in experimental resins in the protein profile of the acquired pellicle formed in situ on enamel-resin specimens, Arch. Oral Biol. (2019), 10.1016/j.archoralbio.2019.104527.

[53]. Ahn SJ, Kho HS, Kim KK, Nahm DS, Adhesion of oral streptococci to experimental bracket pellicles from glandular saliva, Am. J. Orthod. Dentofacial Orthop (2003), 10.1016/S0889-5406(03)00346-9.

[54]. Chi M, Qi M, Lan A, Wang P, Weir MD, Melo MA, Sun X, Dong B, Li C, Wu J, Wang L, Xu HHK, Novel bioactive and therapeutic dental polymeric materials to inhibit periodontal pathogens and biofilms, Int. J. Mol. Sci (2019), 10.3390/ijms20020278.

[55]. Eichler M, Katzur V, Scheideler L, Haupt M, Geis-Gerstorfer J, Schmalz G, Ruhl S, Müller R, Rupp F, The impact of dendrimer-grafted modifications to model silicon surfaces on protein adsorption and bacterial adhesion, Biomaterials (2011), 10.1016/j.biomaterials.2011.08.063.

[56]. Zhang N, Chen C, Melo M.As, Bai YX, Cheng L, Xu H.Hk, A novel proteinrepellent dental composite containing 2-methacryloyloxyethyl phosphorylcholine, Int. J. Oral Sci (2015), 10.1038/ijos.2014.77.

[57]. Müller R, Eidt A, Hiller KA, Katzur V, Subat M, Schweikl H, Imazato S, Ruhl S, Schmalz G, Influences of protein films on antibacterial or bacteria-repellent surface coatings in a model system using silicon wafers, Biomaterials (2009), 10.1016/j.biomaterials.2009.05.079.

[58]. Damodaran VB, Murthy SN, Bio-inspired strategies for designing antifouling biomaterials, Biomater. Res (2016), 10.1186/s40824-016-0064-4

[59]. Siqueira WL, Zhang W, Helmerhorst EJ, Gygi SP, Oppenheim FG, Identification of protein components in in vivo human acquired enamel pellicle using LC-ESI-MS/MS, J. Proteome Res. (2007), 10.1021/pr060580k.

[60]. Cárdenas M, Elofsson U, Lindh L, Salivary mucin MUC5B could be an important component of in vitro pellicles of human saliva: An in situ ellipsometry and atomic force microscopy study, Biomacromolecules (2007), 10.1021/bm061055h.

[61]. Huang R, Li M, Gregory RL, Bacterial interactions in dental biofilm, Virulence (2011), 10.4161/viru.2.5.16140.

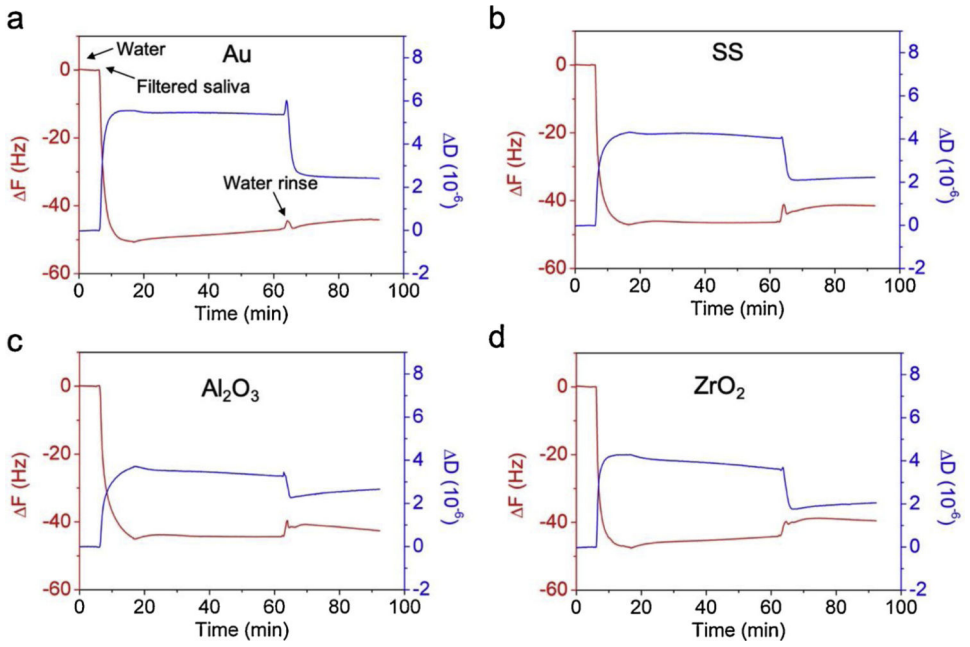

Fig. 1.

Representative QCM-D plots of ΔF (red curve) and ΔD (blue curve) vs time for sensors coated with (a) gold, (b) stainless steel, (c) alumina and (d) zirconia, sequentially exposed to water for system stabilization, FS for formation of salivary pellicle and water for rising attached pellicle (For interpretation of the references to colour in this figure legend, the reader is referred to the web version of this article).

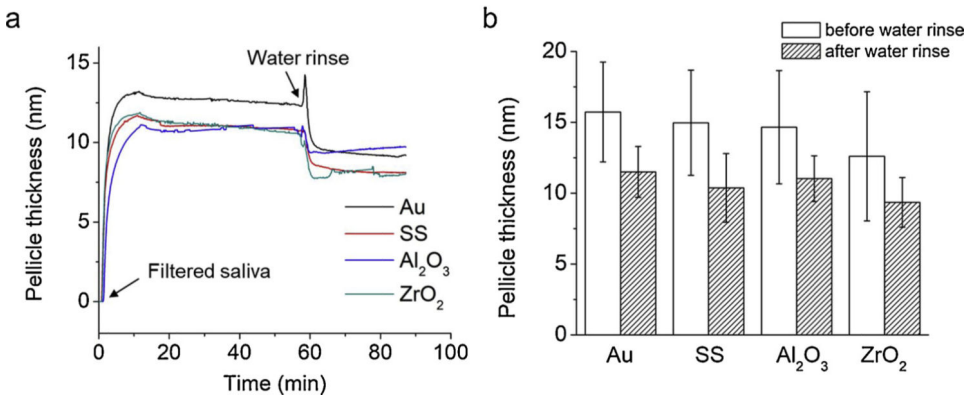

Fig. 2.

Pellicle thickness over time and average pellicle thicknesses formed on four dental materials. Thicknesses were calculated using the Kelvin-Voigt viscoelastic model based on the 5th, 7th and 9th overtones of QCM-D frequency and dissipation changes. No significant differences in thickness were observed for pellicle formed on all four materials, before and after water rinse (N =4).

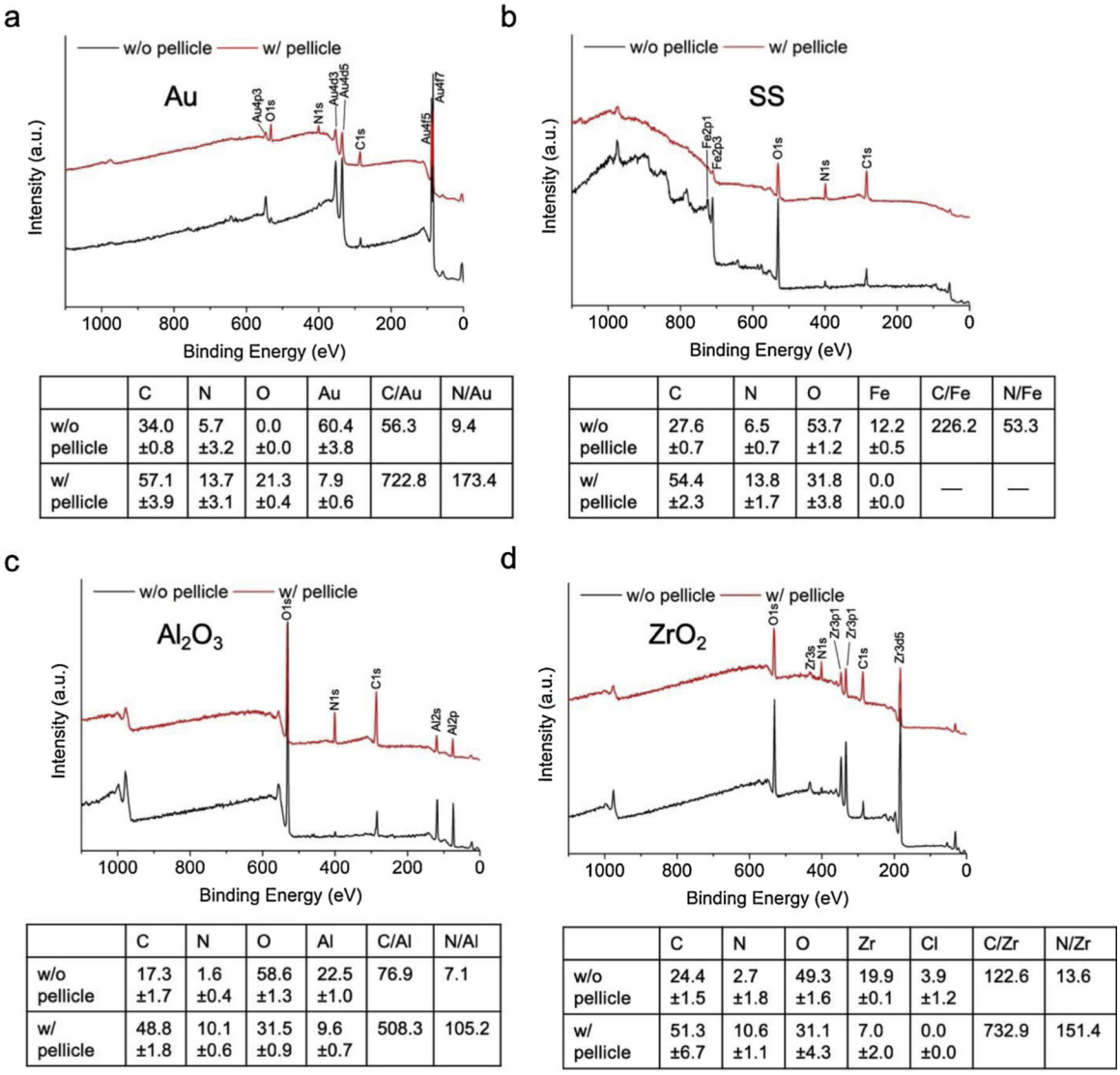

	C	N	O	Au	C/Au	N/Au
w/o pellicle	34.0 ±0.8	5.7 ±3.2	0.0 ±0.0	60.4 ±3.8	56.3	9.4
w/ pellicle	57.1 ±3.9	13.7 ±3.1	21.3 ±0.4	7.9 ±0.6	722.8	173.4

	C	N	O	Fe	C/Fe	N/Fe
w/o pellicle	27.6 ±0.7	6.5 ±0.7	53.7 ±1.2	12.2 ±0.5	226.2	53.3
w/ pellicle	54.4 ±2.3	13.8 ±1.7	31.8 ±3.8	0.0 ±0.0	—	—

	C	N	O	Al	C/Al	N/Al
w/o pellicle	17.3 ±1.7	1.6 ±0.4	58.6 ±1.3	22.5 ±1.0	76.9	7.1
w/ pellicle	48.8 ±1.8	10.1 ±0.6	31.5 ±0.9	9.6 ±0.7	508.3	105.2

	C	N	O	Zr	Cl	C/Zr	N/Zr
w/o pellicle	24.4 ±1.5	2.7 ±1.8	49.3 ±1.6	19.9 ±0.1	3.9 ±1.2	122.6	13.6
w/ pellicle	51.3 ±6.7	10.6 ±1.1	31.1 ±4.3	7.0 ±2.0	0.0 ±0.0	732.9	151.4

Fig. 3.

XPS representative spectra for sensors coated with (a) gold, (b) stainless steel, (c) alumina and (d) zirconia before (w/o pellicle) and after (w/pellicle) pellicle adsorption. Tables show average ± standard deviation (N =4) of element % quantified from the XPS spectra and calculated C/signature metal and N/signature metal for each surface.

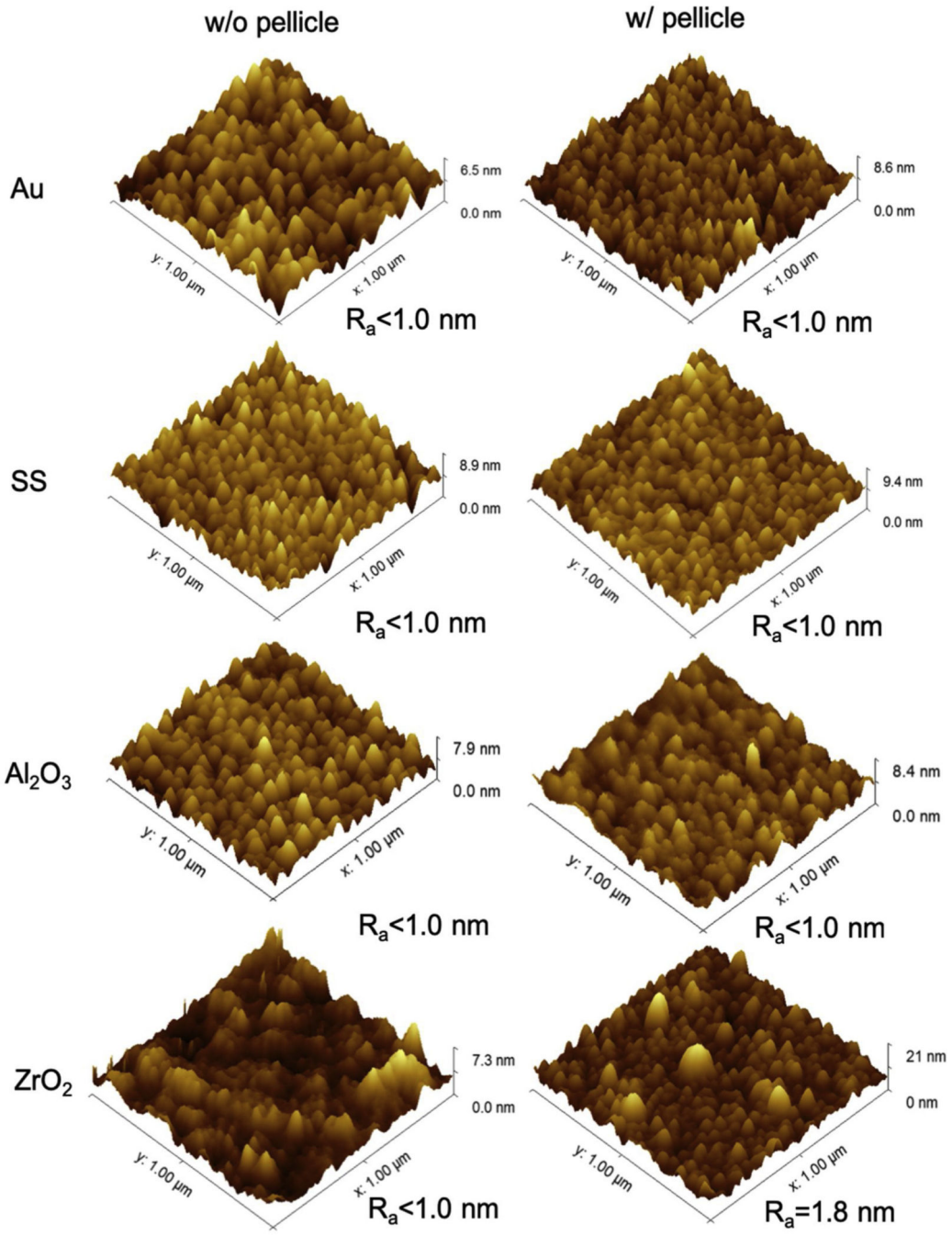

Fig. 4.

AFM images and R_a roughness values for the four sensors without (w/o) and with (w/) pellicle.

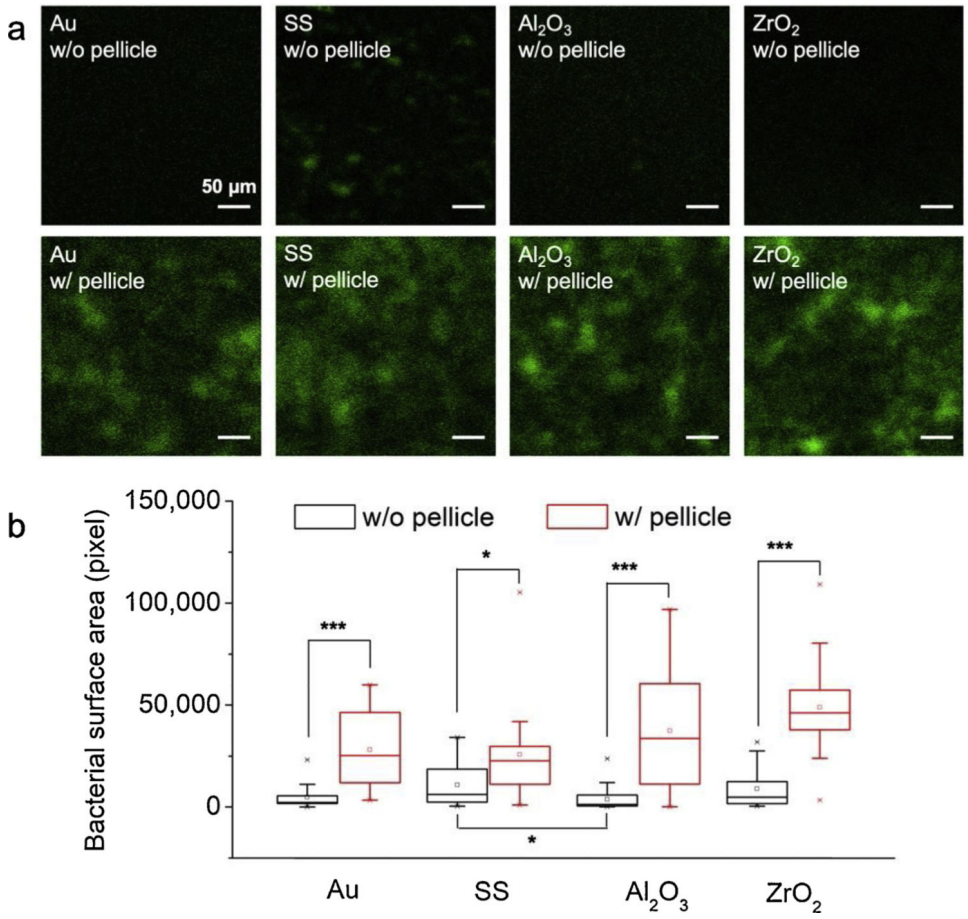

Fig. 5.

Representative CLSM images of bacteria and quantification of surface area covered by bacteria on the different materials before (w/o) and after (w/) pellicle adsorption. * p-value < 0.05, *** p-value < 0.001 (N =4).

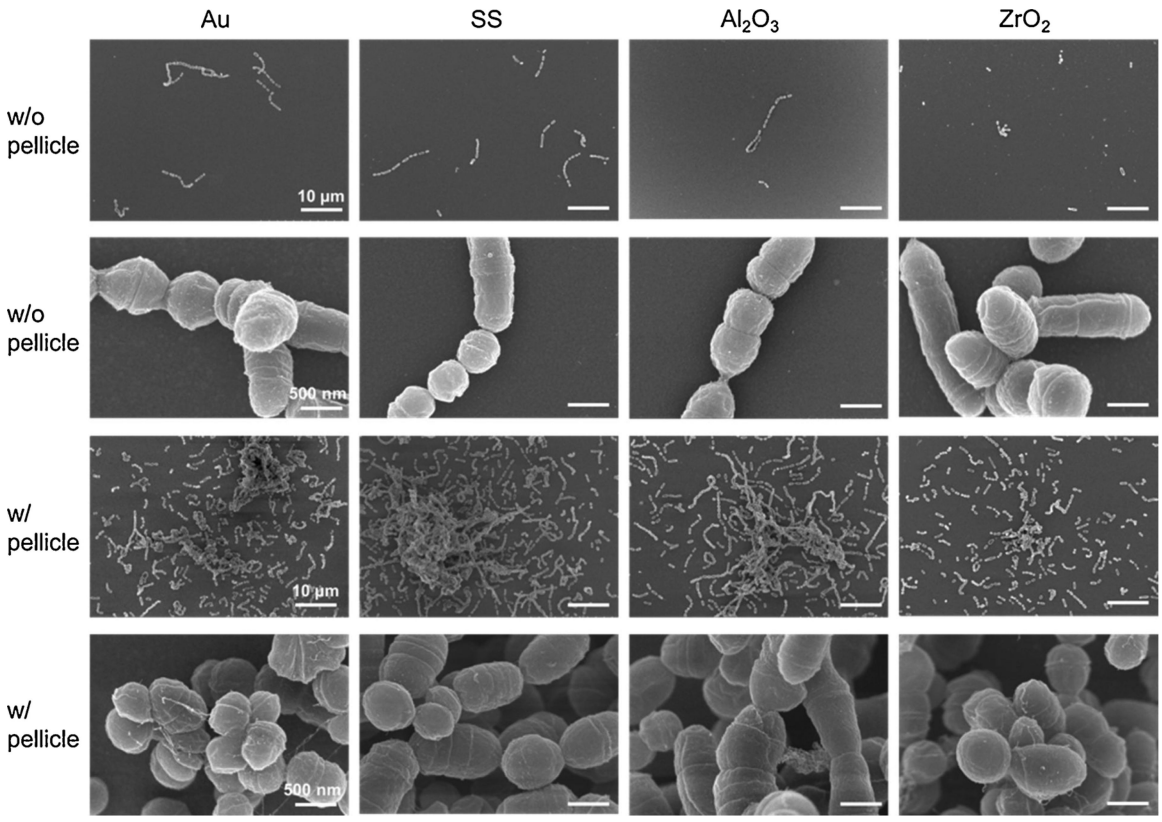

Fig. 6.

Representative SEM micrographs of *S. gordonii* bacteria attached on the four sensors without (w/o) and with (w/) pellicle.

Table 1

Contact angle average ± standard deviation (N = 3) of three liquids (water (WCA), formamide and diiodomethane) and calculated surface energies (γ_{SV}) and their polar $\left(\gamma_S^p\right)$ and dispersive $\left(\gamma_S^d\right)$ components of Au, SS, Al_2O_3 and ZrO_2 sensors, without (w/o) and with (w/) pellicle, and of *S. gordonii layer.* Work of adhesion (W_{ad}) between sensors, without and with pellicle, and *S. gordonii*.

	WCA; Water (deg)	Formamide (deg)	Diiodomethane (deg)	γ_S^p (mJ/m^2)	γ_S^d (mJ/m^2)	γ_{SV} (mJ/m^2)	W_{ad} (mJ/m^2)
Au w/o pellicle	79.0 ± 1.0^{ab,A}	51.6 ± 4.5	432 ± 1.1	5.0 ± 0.5	34.7 ± 1.2	39.7 ± 1.3	76.3
SS w/o pellicle	66.9 ± 5.6 ^{a,A}	60.1 ± 1.5	50.0 ± 0.9	14.1 ± 2.6	24.0 ± 3.4	38.1 ± 4.3	89.5
$A1_2O_3$ w/o pellicle	73.4 ± 22 ^{ab,A}	59.4 ± 1.7	49.1 ± 2.0	9.4 ± 1.2	27.1 ± 1.9	36.5 ± 2.3	82.5
ZrO_2 w/o pellicle	81.1 ± 1.8^{b,A}	57.8 ± 1.6	41.1 ± 1.9	4.0 ± 0.5	34.5 ± 1.4	38.6 ± 1.4	73.0
Au w/ pellicle	48.3 ± 4.2 ^{c,B}	326 ± 6.8	41.9 ± 1.8	25.0 ± 1.9	27.6 ± 1.9	52.6 ± 2.7	109.4
SS w/ pellicle	47.3 ± 1.2 ^{c,B}	34.3 ± 13.3	402 ± 1.0	25.6 ± 2.5	27.3 ± 2.5	52.9 ± 3.5	110.0
Al_2O_3 w/ pellicle	50.2 ± 20 ^{c,B}	36.6 ± 2.3	42.4 ± 1.5	23.9 ± 1.4	27.2 ± 1.4	51.1 ± 2.0	107.6
ZrO_2 w/ pellicle	51.7 ± 1.1 ^{c,B}	320 ± 3.0	41.0 ± 3.6	22.2 ± 0.9	29.0 ± 1.0	51.2 ± 1.3	106.4
S. gordonii	32.9 ± 1.9	27.0 ± 3.4	663 ± 2.0	47.4 ±1.4	14.9 ± 0.8	62.3 ± 1.6	

Lower-case letters next to WCA values indicate statistical significance between different materials, either before (a, b) or after (c) pellicle formation. Upper-case letters next to WCA values indicate statistical significance for each material before and after pellicle formation. Groups with different letters were statistically significant different (p-value < 0.05).